



UNIVERSITY OF
LIVERPOOL

Analysis of the (001) Surface of Ga_3Ni_2 Inter-metallic Catalyst

Alfredo Tarttelin (201454322)

Advisor: Hem Raj Sharma

A thesis presented for the degree of
Bachelor of Science

Department of Physics
University of Liverpool
United Kingdom
26/04/2024

Declaration

I hereby declare that this thesis is my own work and effort and that it has not been submitted anywhere for any award. Where other sources of information have been used, they have been acknowledged.



26/04/2024

ALFREDO TARTTELIN

Acknowledgements

I would like to thank everyone who has supported me with this project with special mentions to Hem Raj Sharma my project advisor who has always given his time to help me and to Oscar Shedwick who provided all the data for this project and helped educate me on all the software needed.

Abstract

Inter-metallic compounds have shown promising properties especially for use as heterogeneous catalysts. They have been found to be more stable and have better selectivity than similar alloy or pure metal catalysts. For an inter-metallic catalyst to be most effective it must be optimised, for this to take place information on the properties is needed. In this project, analysis of the (001) surface of the Ga_3Ni_2 inter-metallic is used to obtain information on the surface structure and chemical composition. Different methods of investigation were completed, these were low energy electron diffraction (LEED), scanning tunnelling microscopy (STM) and x-ray photo-electron spectroscopy. The surface was prepared by sputtering of Argon ions and subsequent annealing. This was completed under ultra-high vacuum conditions. Both LEED and STM showed no signs of reconstruction of the surface. STM also showed step heights that indicate Nickel termination. From XPS it was seen that gallium was preferentially removed from the surface during sputtering and that annealing facilitated diffusion of bulk gallium to the surface. Using the air-exposed and oxidation results it was seen that only Gallium oxidises. Using the STM results and that fact there is no reconstruction it can be said that the catalyst terminates with a nickel plane which is the catalytically active component.

Contents

1	Introduction	3
2	Experimental details	3
2.1	Ultra-high vacuum (UHV)	3
2.2	Surface preparation	4
2.3	Low energy electron diffraction (LEED)	4
2.4	Scanning tunneling microscopy (STM)	5
2.5	X-ray photo-electron spectroscopy (XPS)	6
3	Results, analysis and discussion	7
3.1	Modelling	7
3.2	LEED	8
3.3	STM	10
3.3.1	Step height	10
3.3.2	High resolution	13
3.4	XPS	14
4	Summary	19
5	References	20
6	Appendix	22
6.1	Error equations	22
6.2	STM images	22
6.2.1	Normal	22
6.2.2	High resolution	25
6.3	Data tables	28
6.4	Other diagrams	33
6.5	Literature review, project plan and risk assessment	33
6.5.1	Literature review	33
6.5.2	Project proposal	39
6.5.3	Risk assessment	42
6.6	Presentation questions	47

1 Introduction

Inter-metallic compounds form crystals which are either fully or partially ordered and have a different atomic structure from that of the constituent elements. The unique bonding of inter-metallic (a combination of covalent and ionic) along with the presence of electrons results in exciting combinations of crystal and electronic structures for potential applications as catalysts and in surface chemistry[1]. However, the chemical properties of certain inter-metallic compounds, such as Ga_3Ni_2 has only been scarcely investigated.

Inter-metallic compounds have been found to be attractive candidate for heterogeneous catalysts due to their increased selectivity to specific reactions and their better long-term stability compared to pure or alloyed metals. This increased stability is due to lower heats of formation compared to unordered alloy counterparts and the selectivity is due to the increase in active sites as a result of being ordered[2]. They are of much lower cost as they consist of non-precious metals and therefore can replace precious metal based catalysts[3]. Since heterogeneous catalysis takes place on the surface of materials, high specific surfaces of the inter-metallic compounds are needed that can be achieved by synthesis of nano-particles [4].

The discovery of a Ga–Ni catalysts to facilitate the hydrogenation of CO_2 to methanol at atmospheric pressure [5] is an amazing example of one of these catalysts. With climate change being a particularly large concern world-wide the possibility of having a catalyst and can be a part of green energy fuel cell [5] is exciting. For this catalyst to be optimised, detailed information on its surface is required. Single crystals are needed for the study of the surface and to understand in more detail the catalytic activity. This is due to many of the techniques needing larger single crystal to determine crystal structure of the surface and intrinsic properties[6].

2 Experimental details

All experimental data was taken previous to this project, with this project focusing on the analysis of such. Here the types of analysis and reasons for their use has been described.

2.1 Ultra-high vacuum (UHV)

The experiments were performed in ultra-high vacuum, this is to reduce the contamination, as having an extremely low concentration of contaminants in the chamber, reduces any reaction rate such as oxidation significantly. Ensuring the sample can be as pure as possible, whilst the data is being taken. The UHV is also necessary for data collection as the electrons and photons that the detectors use interact with air which distort any results. The UHV consists of a stainless-steel main body and metal seals. There are 4 pumps in the system: the Turbo pump, with the Rotary as a backing pump, which bring the chamber to a high-vacuum, the ion pump which brings the system into a UHV and the TSP which is a sublimation pump that works to maintain the UHV.

2.2 Surface preparation

For the analytical methods being used a clean surface is required. The single crystal provided was cut and polished with diamond paste however this did leave an oxidation layer caused by air exposure. Obtaining a clean or native surface is important as oxidation also affects the performance of the catalyst as the number of active sites has been reduced[7]. To obtain a clean surface the crystal undergoes ion bombardment of Argon. This leaves a rough surface, to obtain a smoother surface the crystal is then annealed, this is usually below or close to the bulk melting point. This annealing facilitates diffusion of bulk atoms to the surface which removes the defects. It also facilitates the removal of Argon embedded on surface from sputtering. This was completed at different temperatures, so a range of analysis could take place to determine the best temperature to anneal at. This process is commonly referred to as sputter-anneal and is illustrated in Figure 1.

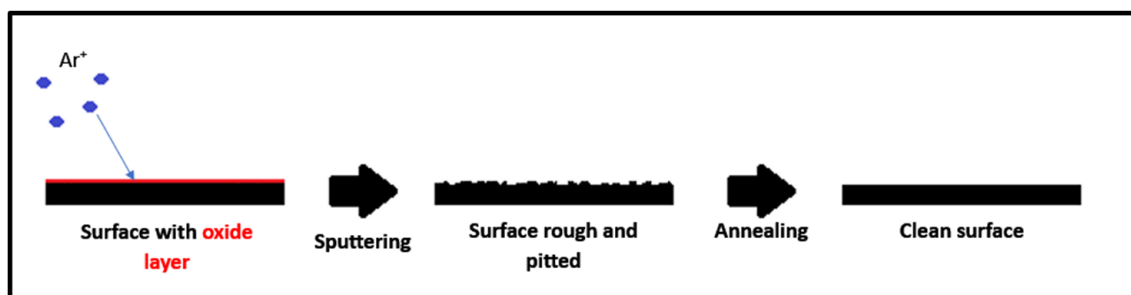


Figure 1: Visual explanation of sputter-anneal.

2.3 Low energy electron diffraction (LEED)

LEED, provides information on the structure and form of the surface, from the LEED pattern which is simply the reciprocal of the conventional lattice. To obtain the pattern electrons emitted from a hot element are accelerated in a drift tube to the required energy before impacting on the sample. The electrons are back-scattered from the crystal's surface in the preferred directions according to the Bragg diffraction conditions. These electrons are collected on a fluorescent screen, which is at a high positive voltage to accelerate electrons to a sufficiently high energy to cause the emission of light, this can be seen in Figure 2. These diffracted electrons produce a pattern of bright spots, this is the LEED pattern, which is recorded by a camera. For LEED to be correctly analysed a calibration with a crystal of a known lattice constant needs to be completed, in this case Al(111) was used. LEED indicates whether a surface has been reconstructed to a different structure than the bulk during the sputter-anneal process. LEED is supplemented with STM for further information on the surface structure[8].

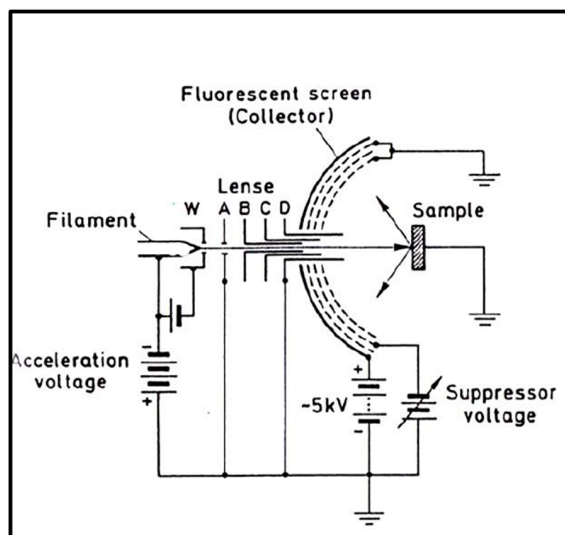


Figure 2: Schematic of LEED [9].

2.4 Scanning tunneling microscopy (STM)

STM can image a surface using a tip. This tip is atomically sharp, meaning there is only one atom at the point. To effectively scan the surface this tip can move in 3-directions with atomic accuracy. Bringing the tip very close to the surface (about 1nm) and applying a bias voltage results in electrons tunnelling through the vacuum barrier due to quantum tunneling. Then by moving the tip across the surface a tunneling current can be measured which is proportional to the local density of state at Fermi level. For the analysis of this crystal a constant current mode was used which keeps the distance between the tip and surface constant. When the tip approaches an edge of a plane the current will change and the tip moves to negate this. There is also an alternative mode, constant height which keeps the height of the tip the same, for this mode a very smooth surface is needed to avoid damaging the tip. A diagram of how STM works can be seen in Figure 3. This tunneling current is then used to create a STM image, these images may then be used to determine the termination of the crystal, which is the composition of the plane that the crystal terminate at or simply what element is on the very top atomic layer.

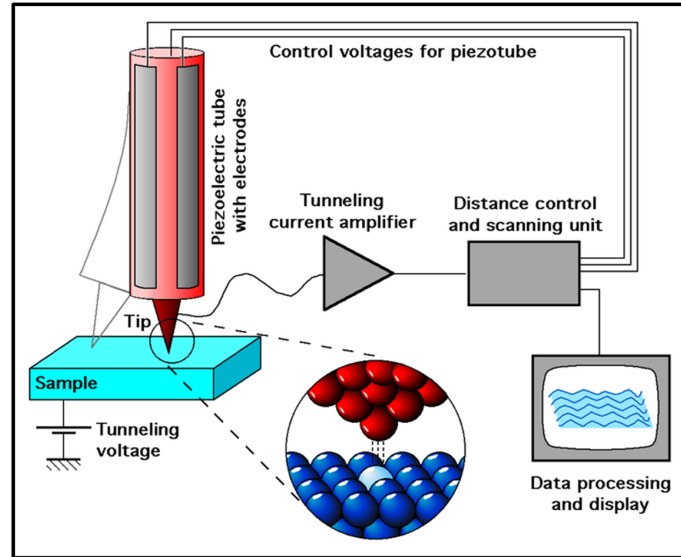


Figure 3: Diagram of STM displaying an atomically sharp tip and a simple circuit showing the tunneling current is both used for distance control and imaging[10].

2.5 X-ray photo-electron spectroscopy (XPS)

XPS which works based on the photoelectric effect can fingerprint elements and provide the chemical composition of the surface. X-ray photons are used to cause electrons to be emitted from the crystal the kinetic energy (E_{kin}) of these electrons is given by equation 1. The kinetic energy is measured using an electron analyser this can be seen in Figure 4. Using known values for the work function ϕ and the energy of the x-ray photons $h\nu$, the binding energy E_b can be calculated. This is used to fingerprint the elements detected as each element has a unique set of core values. Using literature values, the elements on the surface can be identified. Results for XPS were taken before and after sputtering and at the different annealing temperatures.

$$E_{kin} = h\nu - E_B - \phi \quad (1)$$

Where ϕ is the work function, E_b binding energy and $h\nu$ is the energy of x-ray photons.

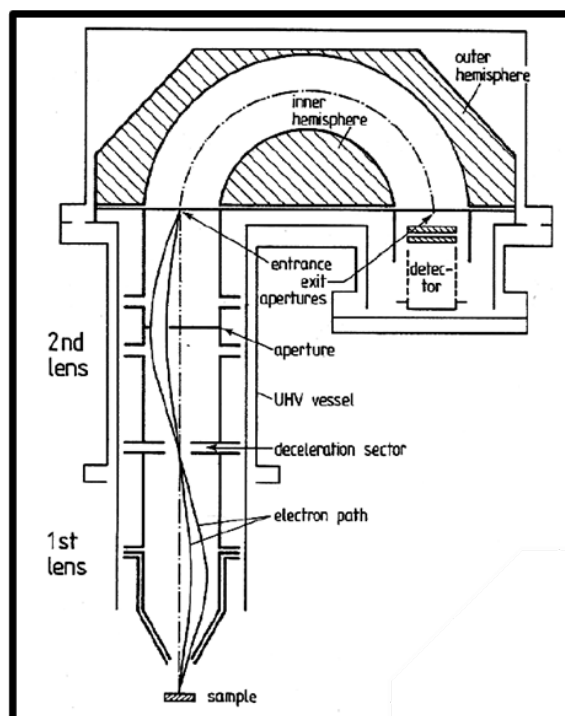


Figure 4: Diagram of XPS, showing the process by which an emitted electron is manipulated so its kinetic energy can be measured using an electron analyser here labelled 'detector' [9].

3 Results, analysis and discussion

3.1 Modelling

Before any analysis took place firstly modelling of the structure of Ga_3Ni_2 was completed. Vesta was primarily used for this[11]. The functions allowed for modelling of the bulk unit cell, (001) surface and the inter-planar spacing of (001) planes. Firstly the bulk unit cell was observed to understand the general structure of the crystal this is seen in Figure 5. Using the lattice parameters measured from the bulk unit and relative directions, the (001) surface and spacing can be identified in relation to the bulk. From the [001] (perpendicular to (001)) view the surface structure can be identified in Figure 6. A measure function was used to extract the lattice constant and shape of conventional cell of the (001) surface, including the angle seen in Figure 6. As it is not currently known what the termination of the crystal is this was completed assuming both gallium and nickle can be the surface layer. However as can be seen in Figure 6 the structure of both of these is the same therefore the surface structure alone will not tell us the termination of the surface. From the [100] (parallel) view, different values for inter-planar spacing between (001) planes (examples indicated by orange boxes) were measured as seen in Figure 7 these different values can help determine the termination of surface as the values for gallium and nickle differ. This is what will be measured from the STM images.

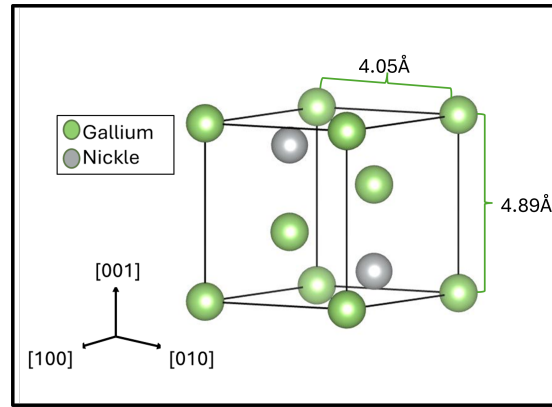


Figure 5: Bulk unit cell of Ga_3Ni_2 with lattice parameters measured and relative directions shown.

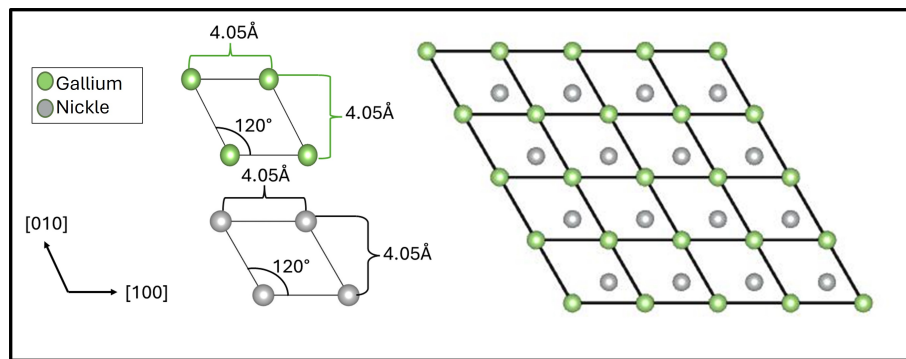


Figure 6: [001] view of the (001) plane of Ga_3Ni_2 with both possible gallium and nickel termination shown alongside their measured rhombus shaped conventional unit cells.

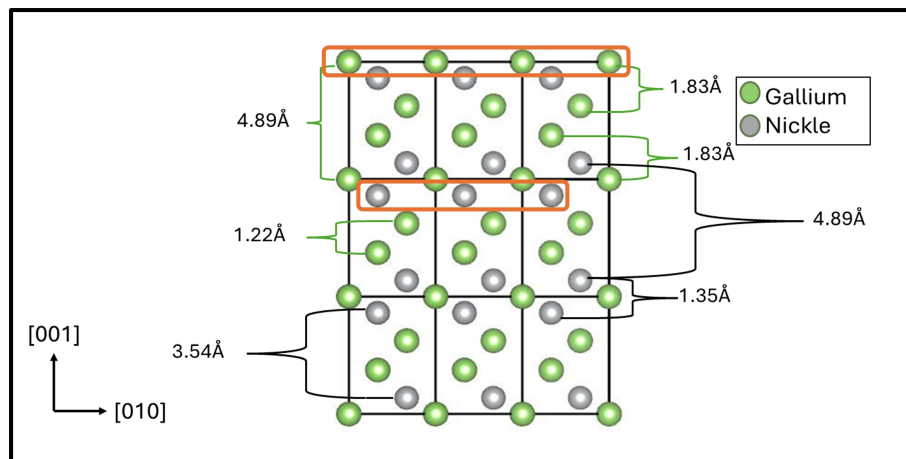


Figure 7: [100] view of the (001) plane of Ga_3Ni_2 showing the different inter planar spacing's for gallium and nickel. With orange boxes indicating potential terminations or (001) planes, any plane parallel to these boxes are also possible.

3.2 LEED

For LEED another piece of software was used for the modelling of a predicted LEED pattern; LEEDpat4. This software required inputs of the lattice constants of a conven-

tional unit cell, the angle between and its shape all of which were provided by the Vesta model in Figure 6. (Note LEEDpat4 defines a rhombus like shape as oblique). As the cells for gallium and nickle are identical their predicted LEED patterns will be identical. To determine the length of a reciprocal unit cell within the LEED pattern, as LEEDpat4 does not provide lengths, equation 2 was used. The model of the LEED pattern and the calculated reciprocal lattice vectors can be seen in Figure 8.

$$A = \frac{2\pi}{a \cdot \sin(\theta)} \quad (2)$$

Where a is the lattice constant, θ is the angle and A is the reciprocal lattice vector.

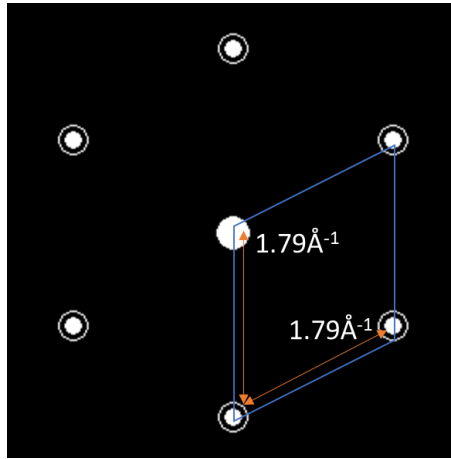


Figure 8: Model of predicted LEED pattern of Ga_3Ni_2 with highlighted rhombus conventional unit cell of reciprocal lattice and annotated reciprocal lattice vectors.

A range of LEED patterns was taken from 0eV to 200eV with a step of 1eV. These images were put together into a gif file. Using a software called ImageJ with the plugin spectra view to easyLEED and inputting the parameters mentioned the gif can be converted into a kind of slide show. Using this its possible to scroll through the LEED pattern at different energies selecting the clearest possible image. The image selected from Ga_3Ni_2 which is in Figure 9 was at 47eV. For the calibration an image of the same energy is required using the same process the 47eV image of Al(111) was extracted and is also seen in Figure 9. These were then both put into the Inkscape software. The images must be of the same 'real' size for measurements to take place. This was done drawing a pink circle around the centre apparatus in the Ga_3Ni_2 and using an exact size copy to adjust and line up the Al(111) image seen in Figure 9.

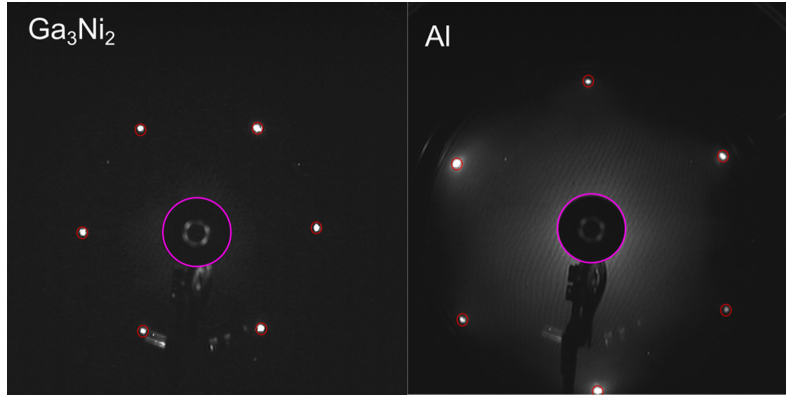


Figure 9: LEED pattern of $\text{Ga}_3\text{Ni}_2(001)$ and $\text{Al}(111)$ at 47eV with the pink circle used to ensure the images are of the same 'real' size. The reciprocal lattice vectors measured in pixels of $\text{Ga}_3\text{Ni}_2(001)$ and $\text{Al}(111)$ is 149.24 and 199.71 respectively.

Using a model of $\text{Al}[12]$ in Vesta and manipulating it for the (111) plane then the conventional cell was found. It was measured and used with equation 2 to calculate the reciprocal lattice vector of $\text{Al}(111)$. This conventional cell can be seen in the appendix.

The reciprocal lattice vector of $\text{Al}(111)$ was calculated to be:

$$A = 2.546 \text{ \AA}^{-1}$$

Using this value to determine the distance per pixel the reciprocal lattice vector of $\text{Ga}_3\text{Ni}_2(001)$ was calculated to be:

$$A = 1.908 \text{ \AA}^{-1}$$

A value relative close to the modelled one in Figure 8. Using this and the fact the pattern for Ga_3Ni_2 in Figure 9 matches the modelled pattern in Figure 8 it can be concluded that there is no surface reconstruction. Meaning after sputter-anneal the surface did not change structure. This shows that the structure of the surface is of that shown in Figure 6 but unfortunately as stated before just knowing this does not establish whether the top layer is gallium or nickel. This is something STM helps to establish.

There are many factors in LEED that can effect the measurement of the reciprocal lattice vector and whilst this does give a close value there are other methods such as STM which uses a wider range of data and can obtain more accurate results. Due to this LEED should only really be used to establish the structure and form of the very top layer and whilst STM is also able to this it take a much longer time.

3.3 STM

3.3.1 Step height

For STM a different software program was required, WSxM [13]. This software allowed for in depth analysis of the STM images. The images display layers or planes and the height difference of these is the step height or inter-planar spacing, a 3D image is shown in Figure 10 where these layers are seen and one measured to show the scale. Two partic-

ular types of analysis were completed for the measuring of step heights: line scans and histograms. An example of the histogram method, which also highlights the flattening required for both histograms and line scan, can be seen in Figure 11 with each of the different colours indicating a plane. For the histogram distance between the peaks is the value of the step height an example measurement can be seen in the histogram in Figure 11. An example of the line scan can be seen in Figure 12 with again the different layers referring to different layers. The line seen in this image crossing over 4 planes and the 3 steps between them measured. These processes were completed across 6 different images which are in the appendix for a total of 122 steps. With the tunnelling current being 0-0.186nA and bias voltage being 0-1V.

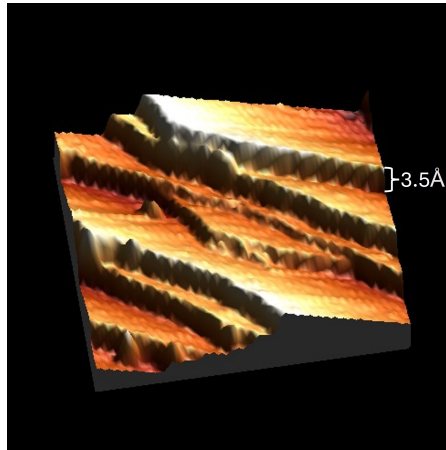


Figure 10: 3D image of an STM scan to show layers of the (001) planes of Ga_3Ni_2 with one measured to indicate scale.

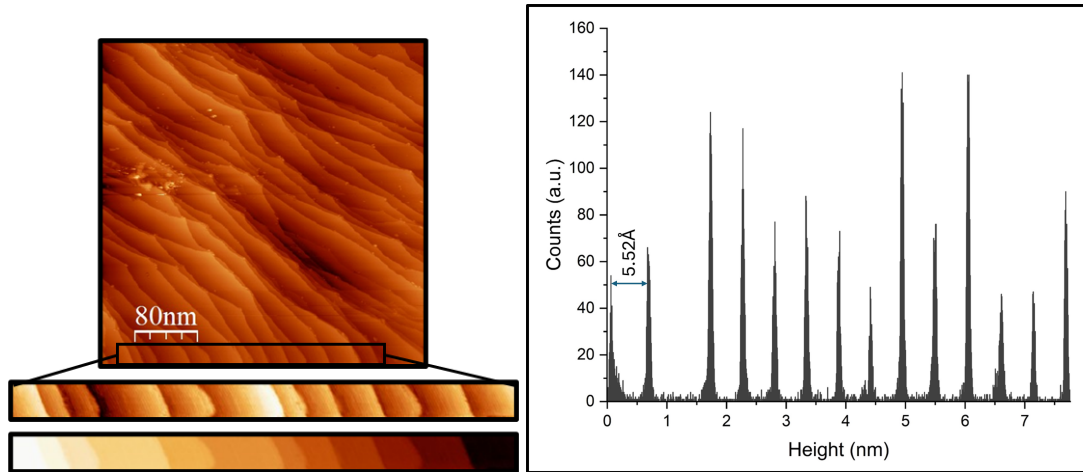


Figure 11: Histogram example of Ga_3Ni_2 (001) inter-planar spacing showing flattening and outputted histogram with an example measurement.

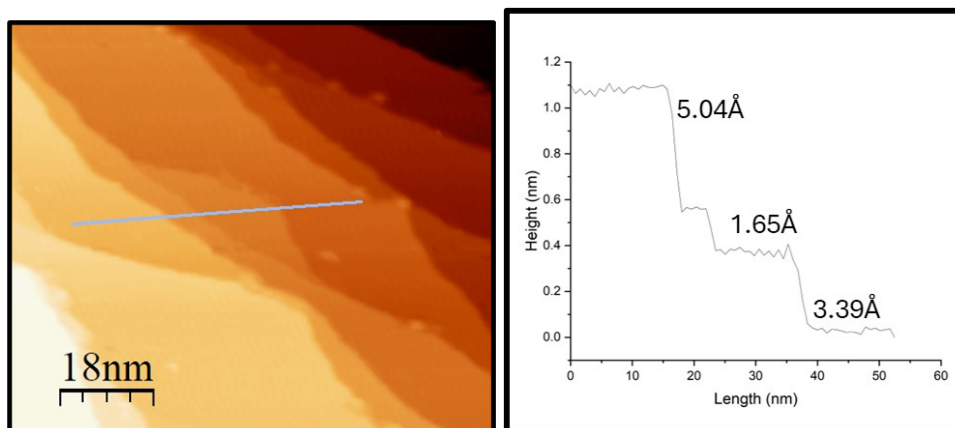


Figure 12: Line scan example of Ga_3Ni_2 (001) inter-planar spacing with measured step heights

To determine the termination at the surface, all the values for the inter-planar spacing were plotted on a histogram and compared with the values from the model in Figure 7. This histogram is seen in Figure 13.

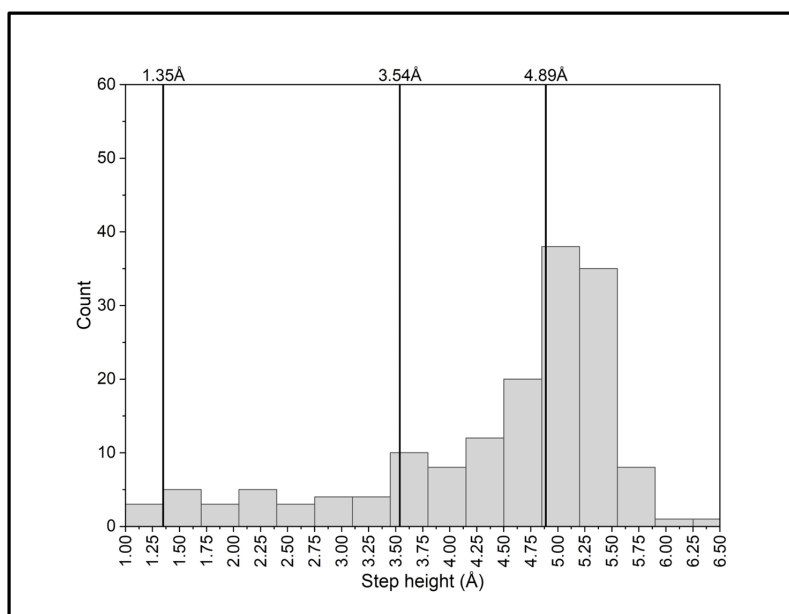


Figure 13: Histogram showing STM inter-planar results of Ga_3Ni_2 with horizontal lines showing predicted model values from Figure 7 assuming nickle termination.

As can be seen in Figure 13 the highest peaks of the histogram line up with the expected model values for inter-planar spacing of nickle from Figure 7. It is also seen from the example line-scan in Figure 12 that the values recorded were relatively consistent with the model values for nickle. Proving that in fact the (001) Ga_3Ni_2 inter-metallic catalyst terminates with nickle planes. This nickle termination is exciting, as nickle is the active catalytic component [7].

If the crystal terminated with Gallium, significant peaks would be expected at 1.83 Å and 1.22 Å due to the model in Figure 7 and this is not the case. There is a significant amount

of results around 5-5.5Å. As the measurements can be taken across a large edge of the step there is a variation in results. There are also issues with small steps, as their small area meant that in both the line scan and histogram analysis it was difficult to get a flat line or sharp peak to obtain a 'good' measurement.

3.3.2 High resolution

Using the Fourier transform function the lattice constant can be extracted from the high resolution images in two ways. The quick method, which is to use the function and simply measure the visible 'LEED' pattern as seen in Figure 14 and then use equation 3 to calculate the lattice constant.

$$a = \frac{1}{k \cdot \sin(\theta)} \quad (3)$$

Where k is the k -vector, a is the lattice constant and θ is the angle between vectors.

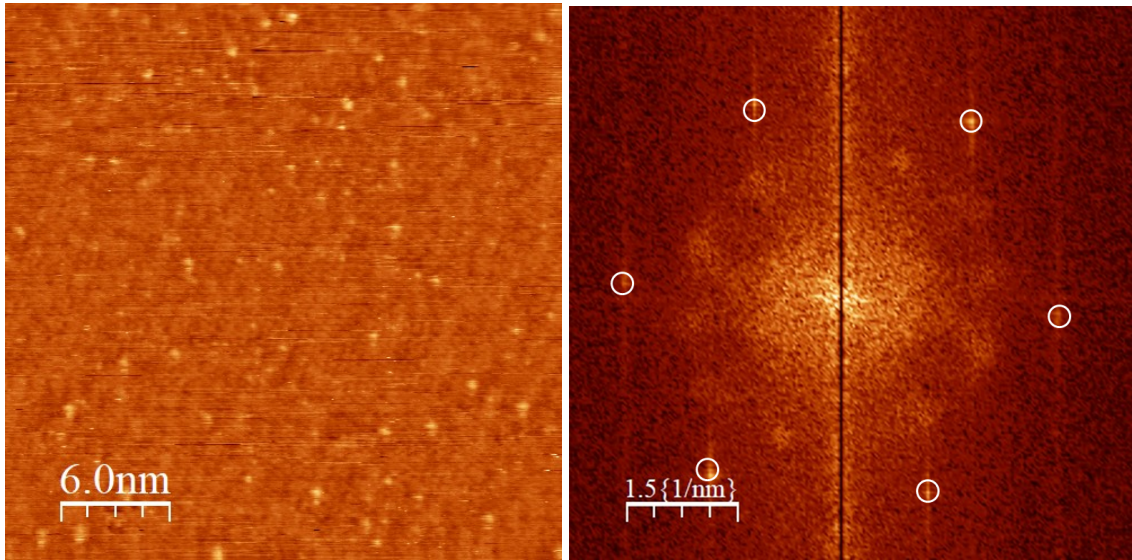


Figure 14: On the left is a High resolution STM image of Ga_3Ni_2 (001) surface with noise removed and flattened. On the right is the Fourier transform of this high resolution image, focused on the 'LEED' pattern with the spots highlighted.

Completing this quick method for 3 images and then taking the average gives the value of the lattice constant from the quick method as:

$$a = 3.94 \pm 0.103 \text{ Å}$$

Focusing the Fourier transform image to only include the spots highlighted in Figure 14 and cutting out everything else an inverse Fourier transform can be plotted that displays the surface structure and can be measured to obtain the lattice constant. An example of this image with the model structure superimposed can be seen in Figure 15.

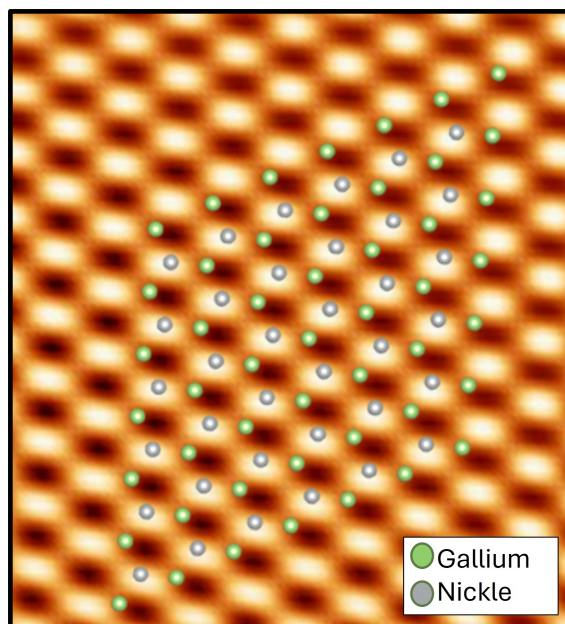


Figure 15: Inverse Fourier transform image with model superimposed to show relevance to surface structure.

Using the same line scan function seen in Figure 12, measurements were taken along the lattice lengths. This method was used for 3 images with 256 lattice lengths measured. Another method of self-correlation where the centre of the Fourier transform in Figure 15 is cut, converted into a high resolution image and the self-correlation function applied was also completed using the same measuring technique however only for 2 images and 22 lattice lengths were measured these were included in the results. An image from self-correlation in the appendix. Taking the average of all the lattice lengths:

$$a = 3.99 \pm 0.21 \text{ \AA}$$

From the FFT data it can be assumed there is no surface reconstruction as the surface seen in Figure 15 with the overlaid image for reference is the same of that of the model. The values found for the lattice constant were relatively close to those shown in the model in Figure 6 however the more in depth method does have a slightly closer value and is based on a much large set of data making it more reliable than the 'quick' value. Some of these images had some blurring to them therefore care had to be taken to select the right regions for measurements to take place to attempt at getting the most accurate results. From the fact the structure matches with the model and that the lattice constants are relatively close to the modelled value it is said that the results agree with the model and that there is no reconstruction of the surface. This confirms the previous result from LEED.

3.4 XPS

For XPS another software program was required this is CasaXPS[14]. This allowed for controlled analysis of XPS data. There were two types of data wide and focused scans. The wide scans provided a good picture of what elements were present after certain

treatments whilst focused scans showed exact peak position core levels and can be used to calculate composition. Two sets of data have been used in the XPS section of this project the first used an aluminium source and the second magnesium. This was due to the fact that after analysis was complete it was seen that there was oxygen present even after sputter-anneal. Therefore a different data set had to be analysed to obtain reliable results. Also due to this, an oxidation result was used. Whilst oxidation results are not a focus of this project, this was used to analyse the oxidation of gallium and nickel. The oxidation process simply uses a clean surface and subjects it to an exposure of pure oxygen measure in units of Langmuir ($1L = 1.6 \times 10^{-6} \text{ mbar} \cdot \text{s}$) for the oxidation data used this was 13300L. A set of wide data scans is shown in Figure 16.

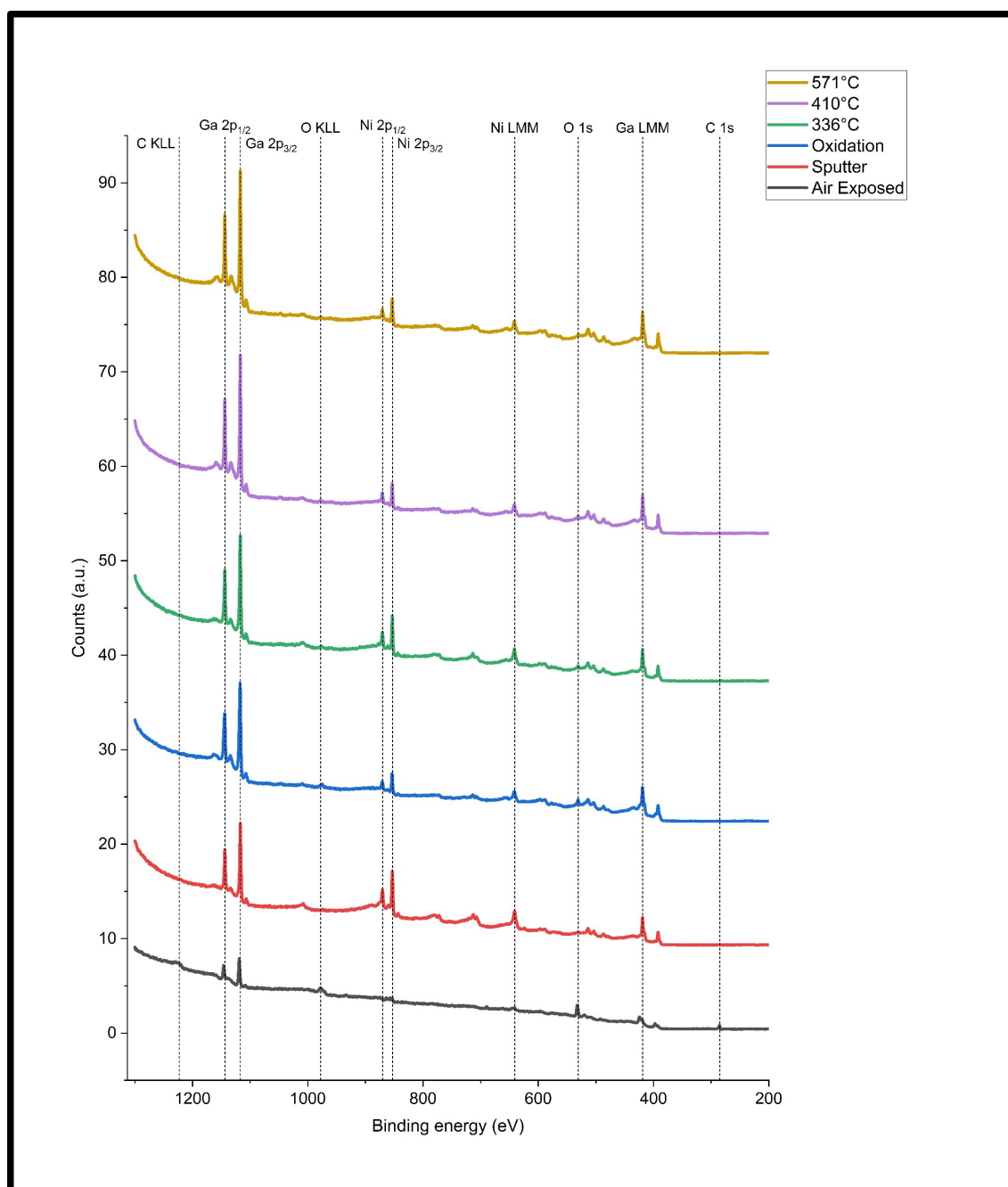


Figure 16: Stacked wide scan XPS with peaks identified from literature core levels [15]

From the wide scans in Figure 16 it can be seen that after sputtering both carbon and oxygen are no longer seen. However a small oxygen peak can be seen in the subsequent annealing temperatures. Proving there was still some oxygen present. However this graph does show very clearly that after sputtering and subsequent annealing the amplitude the gallium peaks increases which would indicate a higher gallium composition to confirm this in depth analysis was required. For this in depth analysis, focused scans of the elements the peaks were fitted. This fitting outputted the peaks' peak position and its area. This was an involved process as with the air exposed and oxidation the peaks recorded could be a combination of two peaks a pure and an oxidised as example of this is shown in Figure 17. For this fitting process the background was defined as Shirley and a function that is combination of Gaussian-Lorentzian was used to fit the peaks.

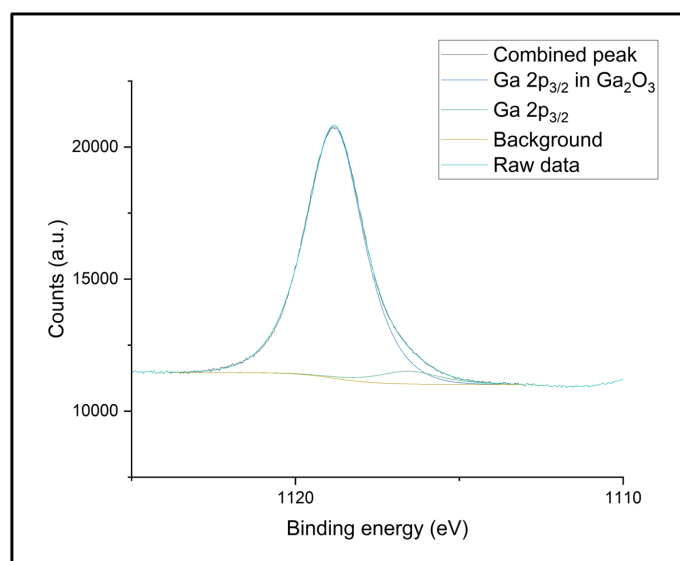


Figure 17: Focused scan of Ga 2p_{3/2} with fitted peaks after air exposure, Shirley background and raw data. Showing how the separate peaks appear as one.

When a set of these peaks is stacked a shift in peak position can be seen, this is plotted in Figure 18 for both gallium and nickle.

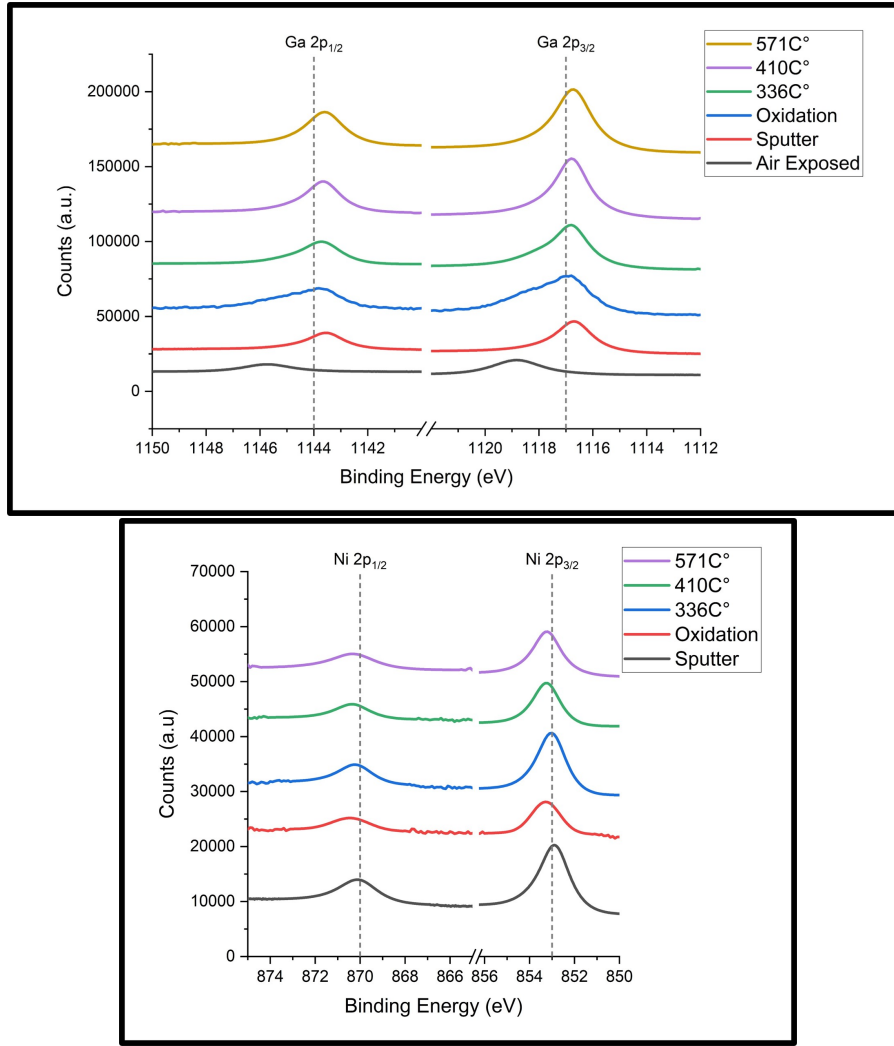


Figure 18: Stacked fitted peaks of XPS showing the peak position shift of gallium and nickel. With clear peak position shift for gallium from air exposed to 571C° annealed.

Extracting the peak position of the different treatments, a table was used to compare to literature values[15].

	Peak Position (eV)				
	Literature	Air Exposed	Sputtered	Oxidised	571C°
Ga 2p _{1/2}	1144	1145.73	1143.53	1143.8	1143.6
Ga 2p _{3/2}	1117	1118.75	1116.68	1116.8	1116.8
Ni 2p _{1/2}	870	N/A	870	870.5	870.2
Ni 2p _{3/2}	853	N/A	852.85	853.2	853.2

Figure 19: Table showing peak positions of various core levels compared to literature values [15]. No air exposed values could be reliably obtained for Nickel hence the oxidation data.

In Figure 19 it can be seen that even after sputtering and annealing at 571C° the values recorded do not match that of the literature. This is because when an element is in a different structure such as an inter-metallic its binding energy can change slightly. This

is also true when an element is oxidised and from the results in Figure 19 this would indicate that gallium may have oxidised as its air exposed results differ to the 571C° annealed value. Extracting the area of the peaks and taking it as the intensity, the chemical composition can be calculated using equation 4.

$$i^{th} \text{ element \% of compound} = 100 \cdot \frac{\left(\frac{I_i}{S_i}\right)}{\sum \left(\left(\frac{I_i}{S_i}\right) + \left(\frac{I_j}{S_j}\right)\right)} \quad (4)$$

Where I is the XPS intensity (area of peak) of either the i^{th} or j^{th} elements and S is the photo-emission cross-section of either the i^{th} or j^{th} elements [16].

With these compositions calculated they were plotted so a comparison of the various treatments of the composition can be seen. Due to the presence of oxygen the composition was plotted twice the plot showing with the contamination can be seen in the appendix. The plotted composition with the clean data is seen in Figure 21. The oxidised data is shown as a table in Figure 20.

Oxidation		
Gallium		Nickle
Oxidised	Pure	Pure
60.69%	2.02%	37.29%

Figure 20: Table of XPS composition Oxidation showing no nickle oxidation.

This oxidation data proves that nickle does not oxidise and in fact only gallium does.

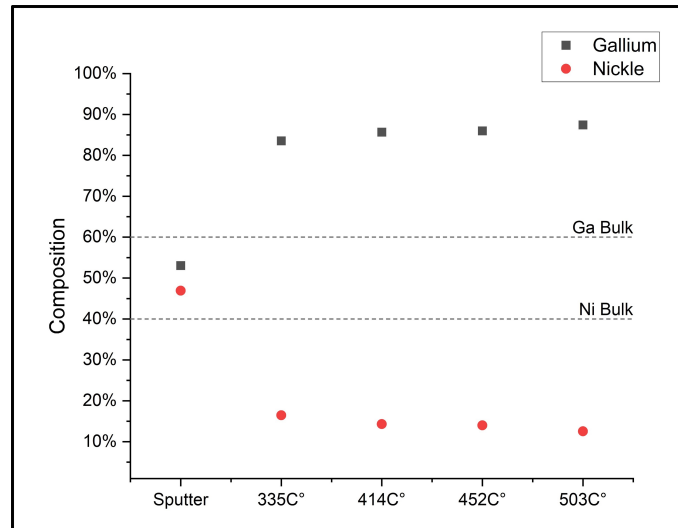


Figure 21: Scatter showing the composition change due to sputtering and increases annealing temperatures with the bulk composition indicated.

From Figure 21 it can be stated that gallium is preferentially removed this is as before

sputtering the composition would be similar to that of the bulk therefore gallium will go from 60% to 53% losing 7% whilst nickel will go from 40% to 47% gaining 7%. Factors that determine preferential removal are the atomic weight, surface free energy and bonding energy. An element will likely be preferentially removed if it has lower values of these factors[17, 18, 19]. It cannot be due to atomic weight as gallium is heavier than nickel however it could be due to surface free energy. The surface free energy of close-packed surface of gallium body-centred tetragonal is 0.661Jm^{-2} whereas close-packed surface nickel face-centred cubic is 2.011Jm^{-2} . From the sputtering result to subsequent annealing it is seen that gallium goes from 53% to 84% and nickel from 47% to 16% and mostly stable as the annealing temperature increases. The increase in gallium composition is due to the annealing process and diffusion of gallium to the surface. This is consistent with nickel being top layer as seen from the model in Figure 7 the nickel layer highlighted by the orange box has 2 subsequent layers of gallium below this can be assumed as there is no reconstruction and as XPS data is of the top few layers the 571C° composition would be consistent with a top nickel layer and 2 gallium layers.

4 Summary

In this project the surface structure and chemical composition of the (001) surface of Ga_3Ni_2 inter-metallic catalyst was investigated using Low energy electron diffraction (LEED), scanning tunneling microscopy (STM) and X-ray photo-electron spectroscopy (XPS). In the first section of this project the surface structure was analysed and there was found to be no reconstruction a result backed up by both LEED and STM. STM step height results were consistent with nickel termination from the model. From XPS it was seen that gallium was preferentially removed from the surface by sputtering and that annealing facilitates diffusion of bulk gallium to the surface. The composition from XPS also backs up the idea of nickel termination. Therefore it can be concluded that the surface most likely terminates with a nickel plane. Which is very useful in the optimisation of the catalyst as nickel is the catalytically active component of Ga_3Ni_2 .

5 References

- [1] M. Armbrüster, R. Schlögl, and Y. Grin. Intermetallic compounds in heterogeneous catalysis—a quickly developing field. *Science and Technology of Advanced Materials*, 2014.
- [2] J. Gamler, H. Ashberry, S.. Skrabalak, and K. Koczkur. Random alloyed versus intermetallic nanoparticles: A comparison of electrocatalytic performance. *Advanced Materials*, 2018.
- [3] M. Armbrüster, K. Kovnir, M. Friedrich, D. Teschner, G. Wowsnick, M. Hahne, P. Gille, L. Szentmiklósi, M. Feuerbacher, M. Heggen, F. Girgsdies, D. Rosenthal, R. Schlögl, and Y. Grin. $\text{Al}_{13}\text{Fe}_4$ as a low-cost alternative for palladium in heterogeneous hydrogenation. *Nature Materials*, 2012.
- [4] M. Armbrüster, G. Wowsnick, M. Friedrich, M. Heggen, and R. Cardoso-Gil. Synthesis and catalytic properties of nanoparticulate intermetallic ga-pd compounds. *Journal of the American Chemical Society*, 2011.
- [5] F. Studt, I. Sharafutdinov, F. Abild-Pedersen, C. Elkjær, J. Hummelshøj, S. Dahl, I. Chorkendorff, and J. Nørskov. Discovery of a Ni–Ga catalyst for carbon dioxide reduction to methanol. *Nature Chemistry*, 2014.
- [6] M. Wencka, M. Pillaca, and P. Gille. Single crystal growth of Ga_3Ni_2 by the czochralski method. *Journal of Crystal Growth*, 2016.
- [7] M. Wencka, J. Kovač, V. Dasireddy, B. Likozar, A. Jelen, S. Vrtnik, P. Gille, H. Kim, and J. Dolinšek. The effect of surface oxidation on the catalytic properties of Ga_3Ni_2 intermetallic compound for carbon dioxide reduction. *Journal of Analytical Science and Technology volume*, 2018.
- [8] A. Ovrutsky, A. Prokhoda, and M. Rasshchupkyna. Structure of the boundary surfaces. *Computational Materials Science*, 2013.
- [9] H. Lüth. *Solid surfaces, interfaces and thin films*. Springer, 2015.
- [10] M. Schmid. Schematic diagram of a scanning tunneling microscope. *TU Wien; adapted from the IAP/TU Wien STM Gallery*, 2005.
- [11] K. Momma and F. Izumi. Vesta3 for three-dimensional visualization of crystal, volumetric and morphology data. *Journal of Applied Crystallography*, 2011.
- [12] M. Fokko, B. Assfour, J. Huot, T. Dingemans., M. Wagemaker, and A. Ramirez-Cuesta. Hydrogen in the metalorganic framework cr mil-53. *The Journal of Physical Chemistry C*, 2010.
- [13] I. Horcas, R. Fernández, J.M. Gómez-Rodríguez, J. Colchero, J. Gómez-Herrero, and A.M. Baró. Wsxn: A software for scanning probe microscopy and a tool for nanotechnology. *Review of Scientific Instruments*, 2007.

- [14] N. Fairley, V. Fernandez, M. Richard-Plouet, C. Guillot-Deudon, J. Walton, E. Smith, D. Flahaut, M. Greiner, M. Biesinger, S. Tougaard, D. Morgan, and J. Baltrusaitis. Systematic and collaborative approach to problem solving using x-ray photoelectron spectroscopy. *Applied Surface Sciences Advances*, 2021.
- [15] J. Moulder, W. Stickle, P. Sobol, and K. Bomben. *Handbook of X-ray Photoelectron Spectroscopy*. Perkin-Elmer Corporation, 1992.
- [16] J. SCOFIELD. Hartree-slater subshell photoionization cross-sections at 1254 and 1487 ev. *Journal of Electron Spectroscopy and Related Phenomena*, 1976.
- [17] L. Feldman and J. Mayer. *Fundamentals of Surface and Thin Film Analysis*. P T R Prentice Hall, 1986.
- [18] P. Sigmund. Theory of sputtering. i. sputtering yield of amorphous and polycrystalline targets. *Phys. Rev.*, 1969.
- [19] D. Jing C. Yuen, B. Unal and P. Thiel. Weak bonding of zn in an al-based approximant based on surface measurements. *Philosophical Magazine*.

6 Appendix

6.1 Error equations

Consistency check: Standard error:

$$\Delta x = \frac{\sigma^2}{n}$$

Where σ is the standard deviation and n is number of data points.

6.2 STM images

6.2.1 Normal

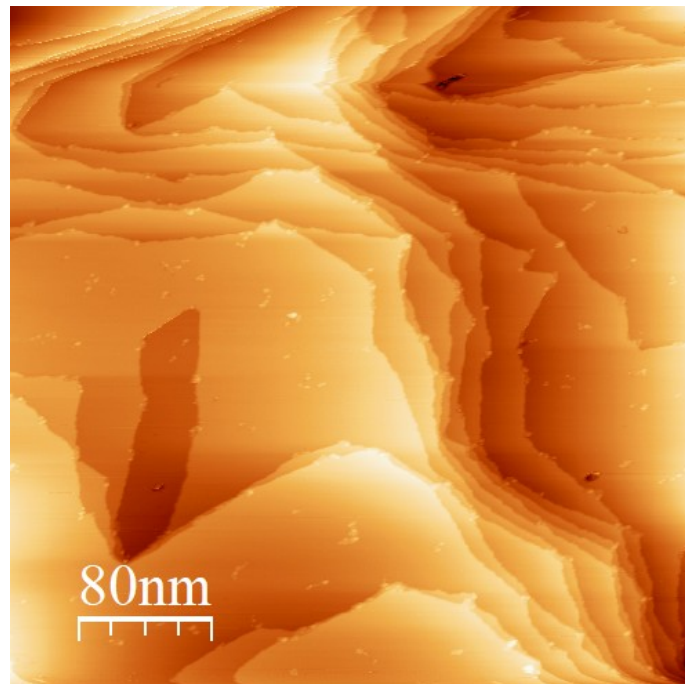


Figure 22: STM Image m1-ori

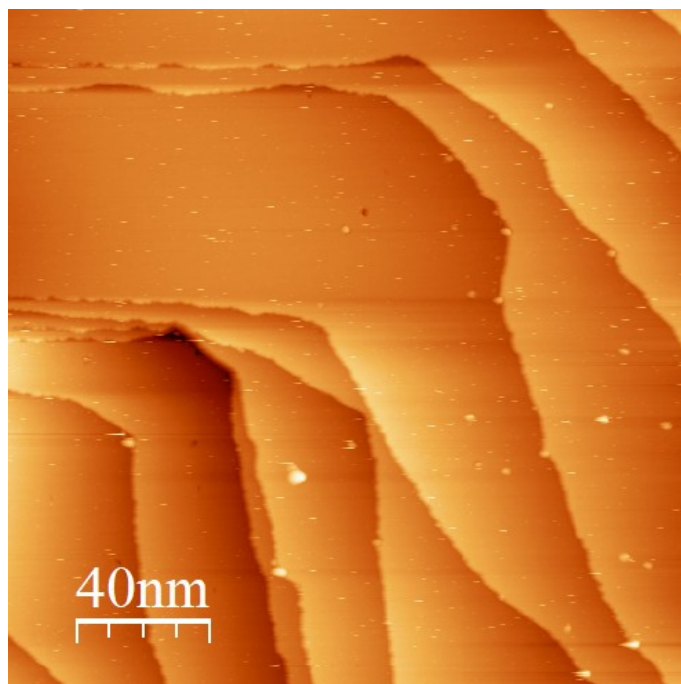


Figure 23: STM Image m1-Z RetraceUp Thu Jun 02 17.26.21 2022 [33-1]

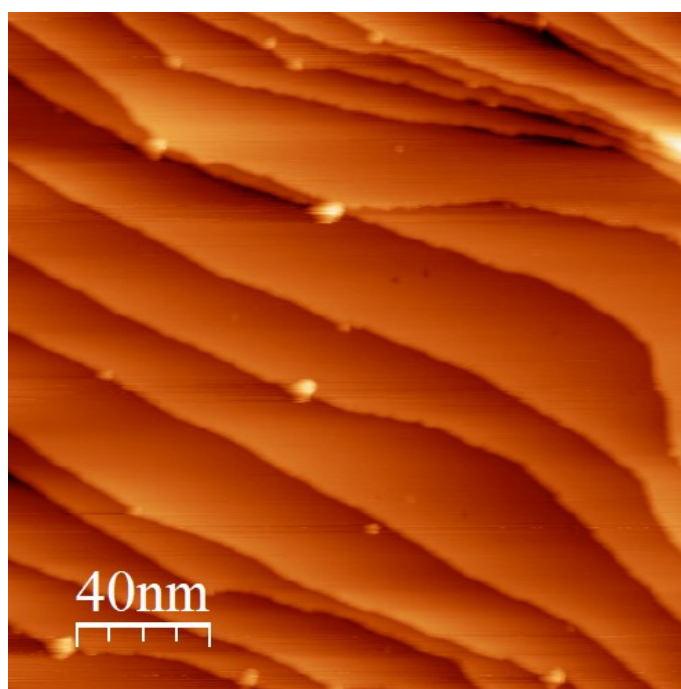


Figure 24: STM Image m1-Z RetraceUp Thu Jun 02 18.09.55 2022 [41-1]

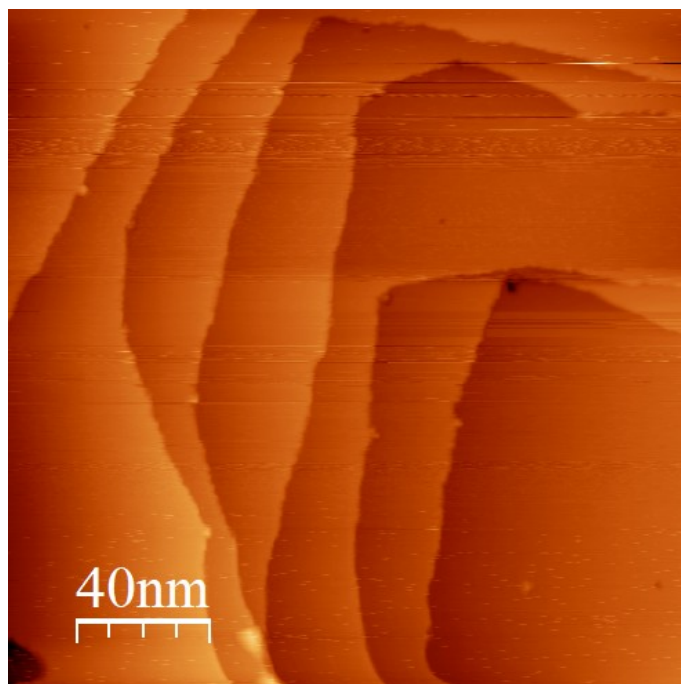


Figure 25: STM Image m1-Z Retrace Up Wed Jun 08 16.20.26 2022 [44-1]

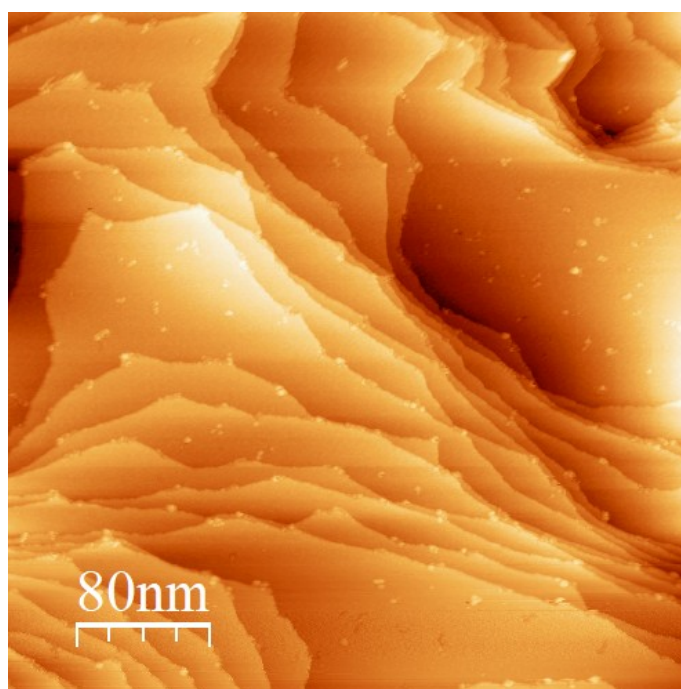


Figure 26: STM Image m5-ori

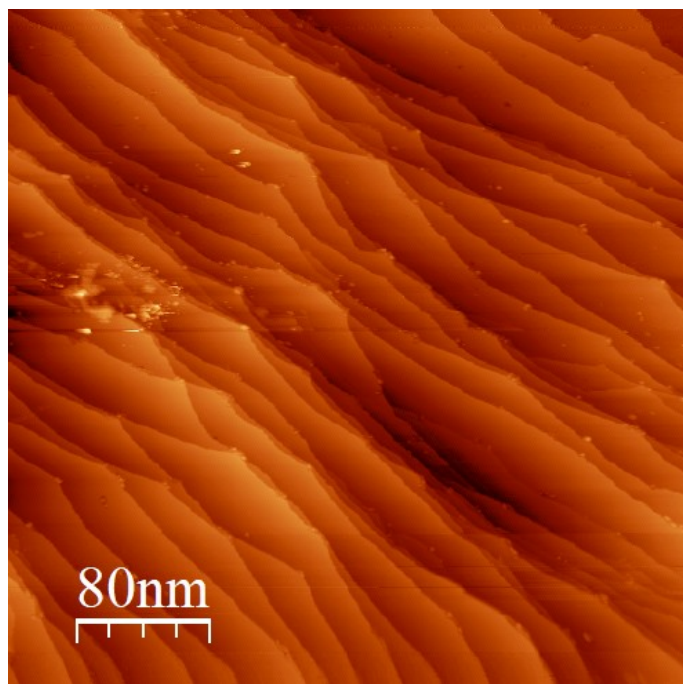


Figure 27: STM Image m6-ori

6.2.2 High resolution

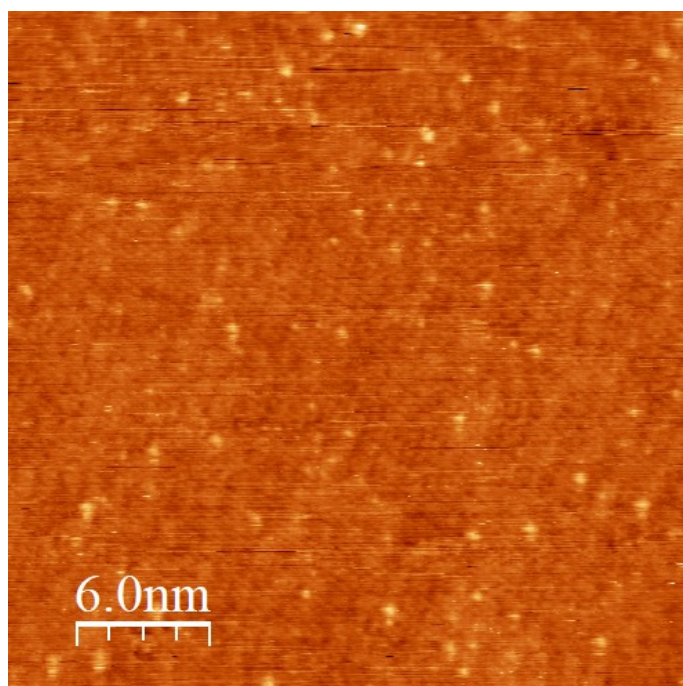


Figure 28: STM High-res Image m1-Z RetraceUp Thu Jun 02 15.15.59 2022 [17-6]

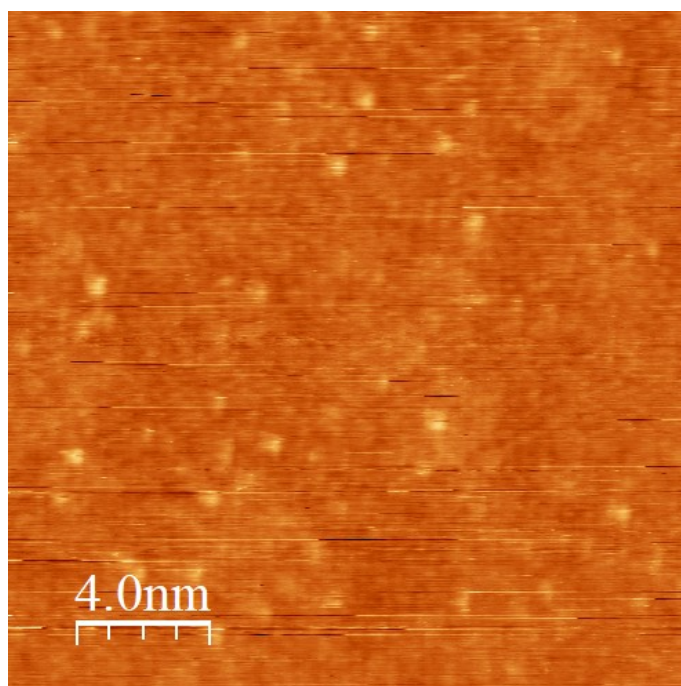


Figure 29: STM High-res Image m1-Z RetraceUp Thu Jun 02 15.23.53 2022 [17-8]

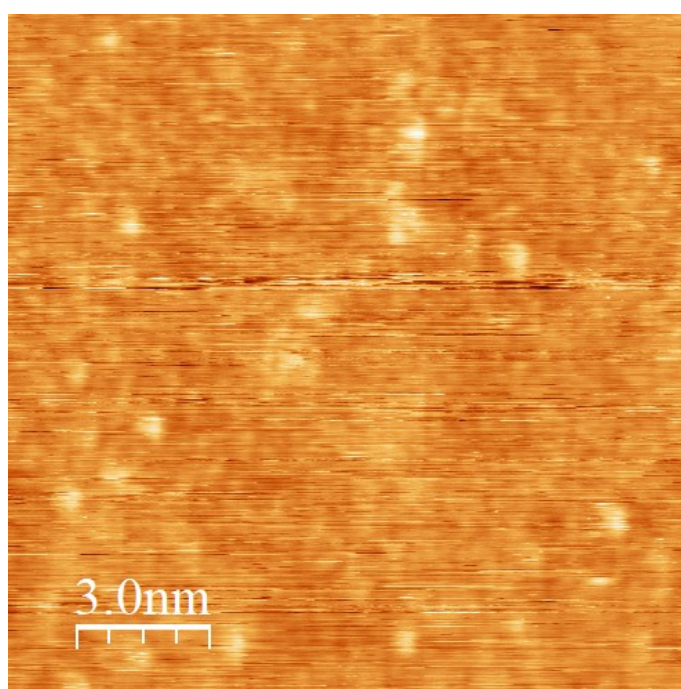


Figure 30: STM High-res Image m1-Z RetraceUp Thu Jun 02 15.31.46 2022 [17-10]

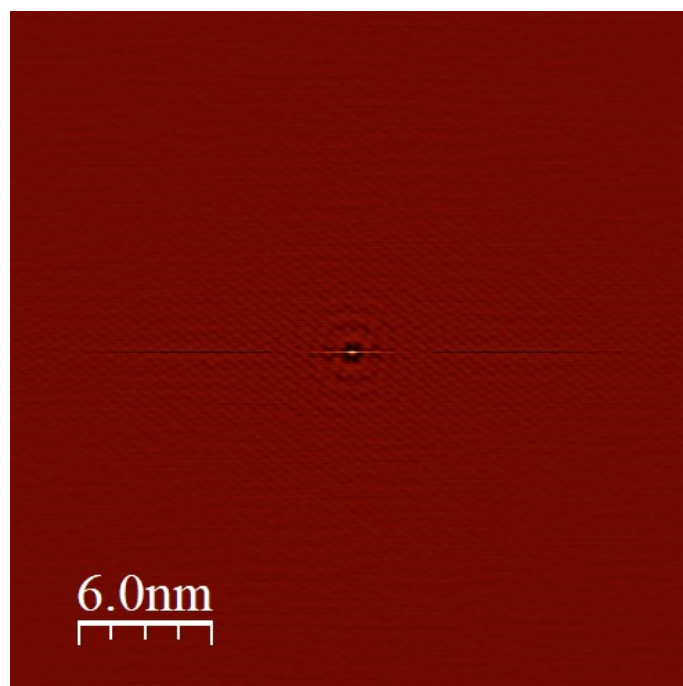


Figure 31: STM self correlation image

6.3 Data tables

Step Height	m1_ori (Å)	m1_Z RetraceUp Thu Jun 02 17.26.21 2022 [33-1] STM_AtomManipulation STM	m1_Z RetraceUp Thu Jun 02 18.09.55 2022 [41-1] STM_AtomManipulation STM	m1_Z RetraceUp Wed Jun 08 16.20.26 2022 [44-1] STM_AtomManipulation STM	m5_ori	m6_ori
1	4.51	4.32	4.651	5.313	4.464	5.24
2	5.495	4.58	5.38	5.247	5.39	5.32
3	4.88	2.032*	6.08	4.753	5.39	5.28
4	4.43	1.19*	4.885	4.948	5.85	5.47
5	4.89	3.135*	5.398	4.656	5.3	5.13
6	3.64	5.173	5.145	4.868	5.48	5.16
7	4.72	4.993	5.195		6.29	5.32
8	4.34	4.795	5.296		5.375	5.09
9	4.34	5.483	4.59		5.504	5.24
10	4.542	4.415	4.858		4.448	5.05
11	5.648		4.986		5.707	5.2
12	4.043		4.949		4.722	5.44*
13	3.62		4.755		5.59	2.88*
14	5.44		4.59		5.31	2.32*
15	4.063		4.97		5.385	5.16
16	4.539		4.969		5.058	4.97
17	3.89				5.3	5.74
18	3.6				5.13	5.03
19	3.26				4.96	5.13
20	4.87				4.394	5.1
21	3.975				5.25	5.19
22					5.259	5.48
23					4.4	5.35
24					4.07	2.96
25					4.16	2.59
26					4.288	2.06
27					4.63	2.73
28					4.62	4.97
29					3.56	2.29
30					3.68	3.85
31						5.17
32						5.13
33						1.52*
34						3.14*
35						5.23
36						5.57
37						5.21
38						5.64
39						5.6

Figure 32: STM step height data.

	Number	Total length	Averaged
m1_Z RetraceUp Thu Jun 02 15.15.59 2022 [17-6] STM_AtomManipulation STM, 'Normal'			
K- vector : 2.940nm ⁻¹ , a = 3.928Å			
Up-down	23	9.104nm	3.958Å
Up-down-2	23	9.109nm	3.960Å
Diagonal SW	24	9.341nm	3.892Å
Diagonal SE	22	8.902nm	4.046Å
"" Self correclation			
	6	2.391nm	3.985Å
	4	1.558nm	3.895Å
m1_Z RetraceUp Thu Jun 02 15.23.53 2022 [17-8] STM_AtomManipulation STM, 'Normal'			
K- vector : 2.964nm ⁻¹ , a = 3.896Å			
Up-down	13	5.205nm	4.004Å
Up-down-2	15	6.065nm	4.043Å
Diagonal SW	13	5.105nm	3.927Å
Diagonal SE	17	6.856nm	4.033Å
"" Self correclation			
	7	2.795nm	3.993Å
	5	1.923nm	3.846Å
m1_Z RetraceUp Thu Jun 02 15.31.46 2022 [17-10] STM_AtomManipulation STM, 'Normal'			
K- vector : 2.983nm ⁻¹ , a = 3.872Å			
Up-down	27	10.967nm	4.062Å
Up-down-2	29	11.713nm	4.039Å
Diagonal SW	28	10.821nm	3.865Å
Diagonal SE	22	9.077nm	4.126Å
"" Self correclation			
	N/A	N/A	N/A
			Total: 3.99Å
			Error: 0.21Å
			Quick Total: 3.94Å
			Error: 0.10Å

Figure 33: STM lattice constant data.

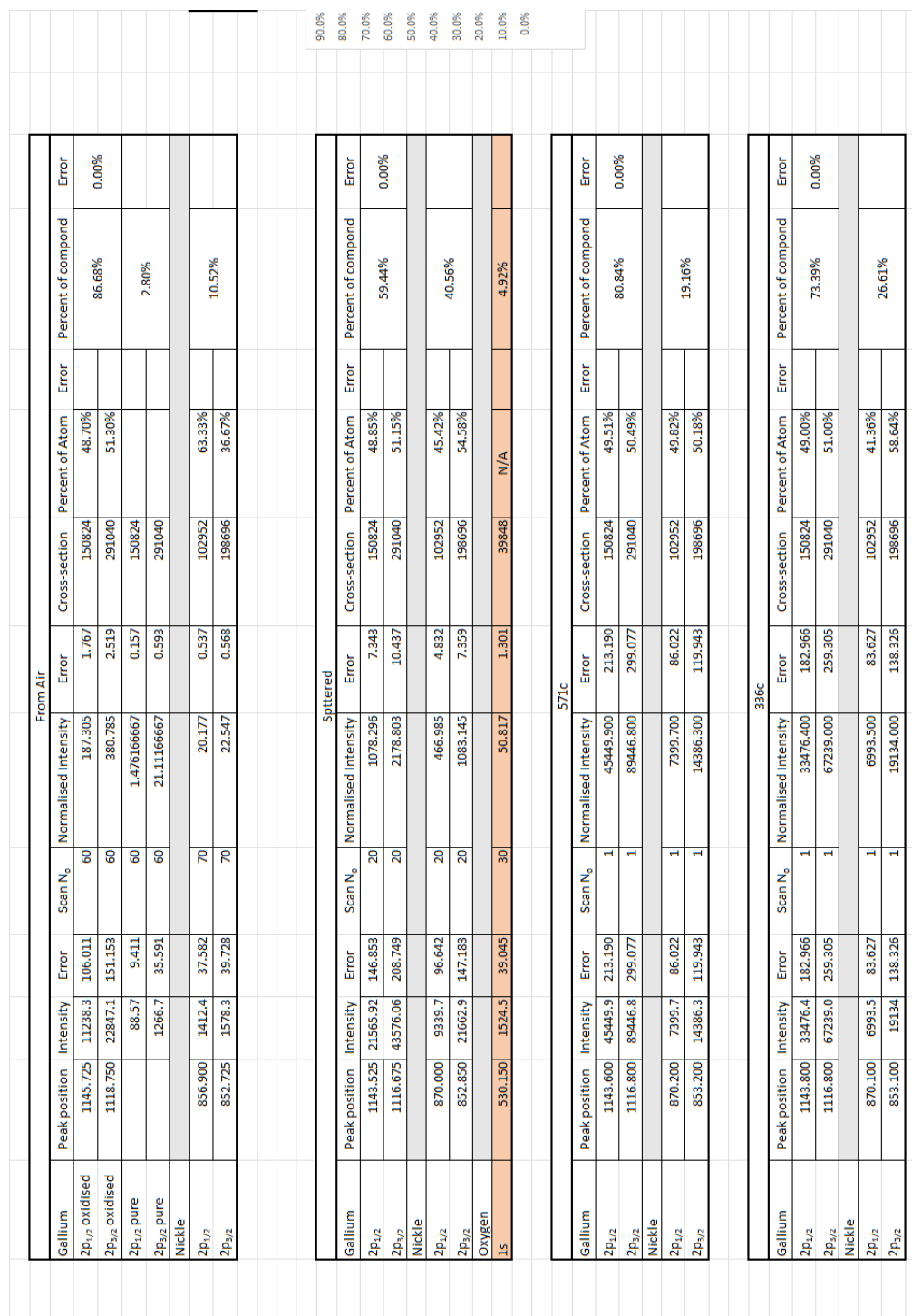


Figure 34: XPS composition data from set 1.

410c									
	Peak position	Intensity	Error	Scan N_0	Normalised intensity	Error	Cross-section	Percent of Atom	Error
Gallium									
$2p_{1/2}$	1143.600	42460.2	206.059	1	42460.200	206.059	150824	66.72%	
$2p_{3/2}$	1116.800	40866.17	202.154	1	40866.170	202.154	291040	33.28%	77.52%
Nickle									
$2p_{1/2}$	870.400	5632.8	75.052	1	5632.800	75.052	102952	44.72%	
$2p_{3/2}$	853.100	13441	115.935	1	13441.000	115.935	198696	55.28%	22.48%
Sputter									
	Peak position	Intensity	Error	Scan N_0	Normalised intensity	Error	Cross-section	Percent of Atom	Error
Gallium									
$2p_{1/2}$	1143.600	56963.35	238.670	2	28481.675	119.335	10.56	45.74%	
$2p_{3/2}$	1116.800	130982	361.914	2	65491.000	180.957	20.47	54.26%	53.07%
Nickle									
$2p_{1/2}$	870.400	32680.6	180.778	2	16340.300	90.389	7.18	43.65%	
$2p_{3/2}$	853.100	81784.99	285.981	2	40892.495	142.990	13.92	56.35%	46.93%
Oxidised									
	Peak position	Intensity	Error	Scan N_0	Normalised intensity	Error	Cross-section	Percent of Atom	Error
Gallium									
$2p_{1/2}$ oxidised		11863.2	108.918	1	11863.200	108.918	150824	48.99%	
$2p_{3/2}$ oxidised		23834.9	154.386	1	23834.900	154.386	291040	51.01%	60.69%
$2p_{1/2}$ pure		23726.4	154.034	1	395.44	154.034	150824		
$2p_{3/2}$ pure		47669.7	218.334	1	794.495	218.334	291040		2.02%
Nickle									
$2p_{1/2}$		5000.2	70.712	1	5000.200	70.712	102952	49.23%	
$2p_{3/2}$		9951.4	99.757	1	9951.400	99.757	198696	50.77%	37.29%

Figure 35: XPS composition data from set 1.

Sputter											
	Peak position	Intensity	Error	Scan No.	Normalised Intensity	Error	Cross-section	Percent of Atom	Error	Percent of compound	Error
Gallium											
2p _{1/2}	1143.600	56963.35	238.670	2	28481.675	119.335	10.56	45.74%		53.07%	0.01%
2p _{3/2}	1116.800	130982	361.914	2	65491.000	180.957	20.47	54.26%			
Nickle											
2p _{1/2}	870.400	32680.6	180.778	2	16340.300	90.389	7.18	43.65%		46.93%	0.01%
2p _{3/2}	853.100	81784.99	285.981	2	40892.495	142.990	13.92	56.35%			
335c											
Gallium											
2p _{1/2}	1143.400	98837.3	314.384	1	98837.300	314.384	10.56	50.21%		83.55%	0.01%
2p _{3/2}	1116.550	189996.4	435.886	1	189996.350	435.886	20.47	49.79%			
Nickle											
2p _{1/2}	870.300	34552.49	185.883	3	11517.497	61.961	7.18	43.69%		16.45%	0.00%
2p _{3/2}	853.1	86325.72	293.812	3	28775.240	97.937	13.92	56.31%			
414c											
Gallium											
2p _{1/2}	1143.400	132155.3	363.532	2	66077.655	181.766	10.56	51.95%		85.69%	0.01%
2p _{3/2}	1116.600	236924.6	486.749	2	118462.320	243.375	20.47	48.05%			
Nickle											
2p _{1/2}	870.450	12726.94	112.814	2	6363.470	56.407	7.18	44.08%		14.31%	0.00%
2p _{3/2}	853.2	31304.91	176.932	2	15652.455	88.466	13.92	55.92%			
452c											
Gallium											
2p _{1/2}	1143.400	135597.3	368.235	2	67798.650	184.118	10.56	51.73%		85.99%	0.01%
2p _{3/2}	1116.600	245248.2	495.225	2	122624.095	247.613	20.47	48.27%			
Nickle											
2p _{1/2}	870.400	11735.19	108.329	2	5867.595	54.165	7.18	40.42%		14.01%	0.00%
2p _{3/2}	853.25	33533.54	183.122	2	16766.770	91.561	13.92	59.58%			
502c											
Gallium											
2p _{1/2}	1143.450	351434.5	592.819	5	70286.898	118.564	10.56	52.67%		87.45%	0.01%
2p _{3/2}	1116.600	612227	782.449	5	122445.398	156.490	20.47	47.33%			
Nickle											
2p _{1/2}	870.400	29019.9	170.352	5	5803.980	34.070	7.18	44.57%		12.55%	0.00%
2p _{3/2}	853.25	69961.98	264.503	5	13992.396	52.901	13.92	55.43%			

Figure 36: XPS composition data from set 2.

6.4 Other diagrams

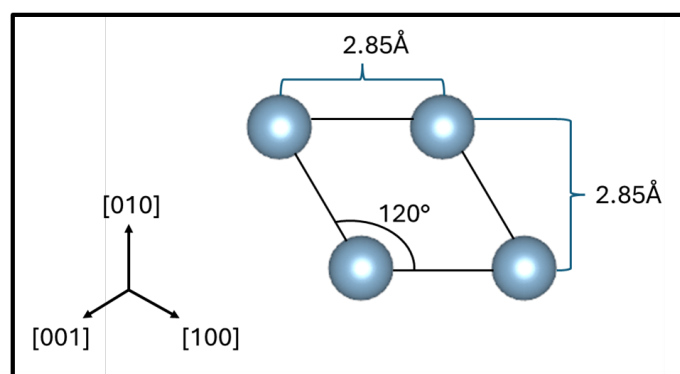


Figure 37: Model of Al(111)

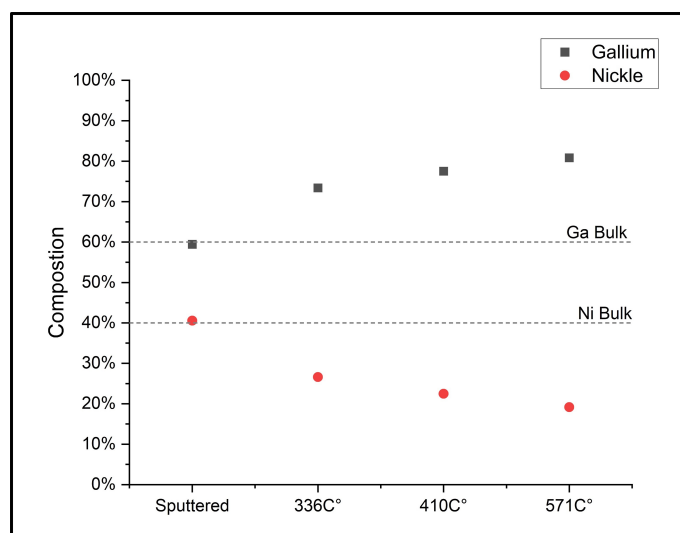


Figure 38: Composition from XPS of contaminated data

6.5 Literature review, project plan and risk assessment

6.5.1 Literature review

Literature Review

Alfredo Tarttelin (201454322)

Advisor: Hem Raj Sharma

Department of Physics, University of Liverpool

05/04/2024

1 Introduction

1.1 Background

Climate change is a very pressing issue in today's world especially the presence of CO₂ in the atmosphere as a result of combustion. Inter-metallic catalysts is a developing area which could provide solutions to these problems not only as they have unusual bonding and scarcely investigated chemical properties but they are also constructed of non-precious metals greatly reducing any costs.[1] The discovery of a Ga-Ni catalyst that facilitates the hydrogenation of CO₂ to methanol could be one of these solutions.[2] This is as the crystal could be used in a fuel cell which is carbon neutral.

1.2 Objective

In this project the Ga₃Ni₂ crystal surface will be investigated, data from this can be used to optimise its use as a catalyst. For this investigation a single crystal is required, several techniques are used LEED, XPS and STM. This literature review will look into the existing text on the Ga₃Ni₂ crystal and the techniques being used.

2 Discussion of literature

This section will detail the main sources of research including the inspiration for this project. This should give some context and outline the motivation.

2.1 Source 1 [2]

This academic paper was written by 8 physicists and published in Nature Chemistry. A Ni-Ga crystal was discovered to be a catalyst in the reduction of CO₂ to methanol at ambient pressure. Three Ni-Ga crystals were analysed Ni₃Ga, Ni₅Ga₃ and NiGa. These catalysts were not optimised. It also outlines the potential use of the crystal for green energy particularly a fuel cell and the fact the catalyst is based on non-precious inexpensive metals. Issues that could arise and that need to be analysed are the potential poisoning of the catalyst in the environment.

2.2 Source 2 [3]

This academic paper was written by 3 physicists and was accepted into the Journal of Crystal Growth. The report focuses on the fact that heterogeneous catalysts which contain precious metals are expensive and that inter-metallic crystals have increased selectivity to specific reactions and their better long-term stability compared to pure or alloyed metals. It also details the discovery in Source 1 and that Ga₃Ni₅ is a particularly active and selective catalyst but cannot be grown from a binary liquid phase. There is only one line compound of fixed stoichiometry, namely Ga₃Ni₂ that is in equilibrium with a binary Ga-Ni melt. Its catalytic activity has not been tested so far in the published study [2] single crystals are not necessary for industrial use they are needed for surface analysis. Whilst the for the first time cm-size single crystals of the binary inter-metallic compound Ga₃Ni₂ were grown. High-temperature solution growth using the Czochralski technique.

2.3 Source 3 [4]

This academic paper was written by 9 physicists and was accepted into the Journal of Analytical Science and Technology. Air-exposure can be an issues for many materials, therefore the effect of air exposure on the inter-metallic catalyst has been analysed. This was done using the x-ray photo spectroscopy (XPS) method. XPS gives elemental composition and chemical bonding (oxide or metal) useful to determine the composition of oxide on the surface. It is found that air-exposure does oxidise the surface this oxide reduces the number of active sites and therefore the performance of the catalyst. To remove an oxide layer sputtering is used followed by annealing. However depth of sputtering and temperature of annealing are important factors. The XPS analysis is done both pre and post sputter-annealing and in a ultra-high vacuum (UHV) this reduces any reactivity time to longer than any acquisition time. It was observed that an annealing temperature of over 300°C is needed and that there is increased conversion at 600°C

2.4 Inter-metallic catalysts [1]

Inter-metallic compounds form crystals which are partially or fully ordered and different from constituent elements. The unusual bonding of combinations of ionic and covalent with the presence of conducting electrons results in attractive combinations of crystallographic and electronic structures for potential applications in catalysis and surface chemistry. So far, the chemical properties of inter-metallic compounds are only scarcely investigated. due to the developing field of these 'Inter-metallic catalysts' and large single crystals. This paper was written by 3 physicist and published into Science and Technology of Advanced Materials.

2.5 Low energy electron diffraction (LEED)

LEED is used to analyse the surface structure and can be used with most materials including inter-metallic compounds. LEED requires surface preparation such as sputtering and annealing. Professionally written and published in NATO ASI Science..[5]

LEED patterns display the reciprocal lattice. As the LEED method does not reveal arrangement of atoms in cells of the surface crystalline structure it is supplemented with other techniques such as electron microscopy e.g. STM. Written by 3 physicists and published in Computational Materials Science.[6]

2.6 Scanning tunneling microscopy (STM)

STM can create an atomically accurate image of a surface using an atomically sharp tip. STM data requires detailed analysis unlike LEED. Due to its unique features manipulation on the atomic scale is being explored, such as determining the catalytic surface. The surface must be clean for analysis to take place using sputter-anneal and UHV. Written by 4 physicists and published Surface Science Reports no reason to doubt.[7]

There are two methods to STM constant height and constant voltage. Constant height has the issue where is the surface is not completely flat the tip can collide with the surface damaging the tip and corrupting any further data. Constant voltage keeps the tunneling voltage constant i.e the distance between the tip and surface. Advantages of constant height being that the acquisition is much quicker. [8]

3 Analysis

As this is a relatively new area of investigation there is not much in the way of any conflicts. The area has many papers being published constantly building on each

others work and refining it. One issue is that this crystal in particular has not been widely researched therefore there is not data there to go through especially with the surface analysis of Ga_3Ni_2 where other than Source 3 there is nothing. Some of the authors of the papers are the same as stated before this is a new research area so simply there is not many people involved this could be taken as a potential area for mistrust but these are all scientists with extensive qualifications and furthermore all these papers have been published into journals the process of which includes peer review and scrutiny. This is the same for papers mentioned.

4 Conclusion

Bias is not something seen greatly in scientific papers due to the peer review and scrutiny to get published in a journal. To provide more insight on why these are unbiased is due to the abundances of data provided in these reports along with the language used, which simply states previous findings, data and the clear conclusions that can be drawn from these. With all these reasons I can say the information I have taken from these sources is unbiased, consequently my review is unbiased.

All this information greatly corresponds to my project and helps give context to it. The project is analysing the surface of Ga_3Ni_2 to optimise use of the catalyst described in Source 1. For this analysis a single crystal is needed, the same crystal described in Source 2. The analytical methods used are common place in the research area, the papers I used for these help described why these methods are being used, due to the data they provide and the necessity of the conditions. This literature review will help me understand the reasons for each method and the motivation for the research taking place. It also outlines that inter-metallic catalysts surfaces have only scarcely investigated giving reason to the lack of data available.

5 References

- [1] Robert Schlögl Yuri Grin Armbrüster, Marc. Intermetallic compounds in heterogeneous catalysis—a quickly developing field. *Science and Technology of Advanced Materials*, 2014.
- [2] Frank Abild-Pedersen Christian F. Elkjær Jens S. Hummelshøj Søren Dahl Ib Chorkendorff Jens K. Nørskov Felix Studt, Irek Sharafutdinov. Discovery of a Ni–Ga catalyst for carbon dioxide reduction to methanol. *Nature Chemistry*, 2014.
- [3] Peter Gille Magdalena Wencka, Mirtha Pillaca. Single crystal growth of Ga_3Ni_2 by the czochralski method. *Journal of Crystal Growth*, 2016.
- [4] Venkata D. B. C. Dasireddy Blaž Likozar Andreja Jelen Stanislav Vrtnik Peter Gille Hae Jin Kim Janez Dolinšek Magdalena Wencka, Janez Kovač. The effect of surface oxidation on the catalytic properties of Ga_3Ni_2 intermetallic compound for carbon dioxide reduction. *Journal of Analytical Science and Technology volume*, 2018.
- [5] M. A. Van Hove. Low-energy electron diffraction and electron holography: Experiment and theory. *NATO ASI Science*, 1992.
- [6] M.S. Rasshchupkina A.M. Ovrutsky, A.S. Prokhoda. Structure of the boundary surfaces. *Computational Materials Science*, 2013.
- [7] Nobuyuki Isshiki b Hiroyuki Kageshima a 1 Masaru Tsukada a, Katsuyoshi Kobayashi a. First-principles theory of scanning tunneling microscopy. *Surface Science Reports*, 1991.
- [8] S. Vinzelberg G. Staikov W.J. Lorenz J. Halbritter a, G. Repphun. Tunneling mechanisms in electrochemical stm —distance and voltage tunneling spectroscopy. *Electrochimica Acta*, 1995.

6.5.2 Project proposal

Project Proposal

Alfredo Tarttelin 201454322

Project: Surface Atomic Structure of Ga_3Ni_2 and In_3Ni_2 Intermetallic Catalysts

Supervisor: Hem Raj Sharma

Main Aims and Objectives:

In this project the surfaces of Ga_3Ni_2 and In_3Ni_2 will be investigated. As understanding the surface structure and electronic properties is important to optimise catalytic activities. (These crystals are used as catalysts.)

To investigate the surface atomic structure, low energy electron diffraction (LEED) and scanning tunneling microscopy (STM) will be used.

To investigate the surface chemical composition and oxidation (electronic properties); X-ray photoelectron spectroscopy (XPS) will be used.

The surface sample used is prepped before any data can be taken the process of which should be researched and documented. Part of this process uses an ultra-high vacuum.

Timeline for Project	
Starting 06/11/2023 (S1 Week 7) Project proposal due: (10/11/2023)	Hand in project proposal.
(S1 Week 8)	Researching preparation of surfaces, the surfaces themselves, ultra-high vacuum and the different types of data taking (LEED, STM and XPS) Discussion with Phd student and advisor on how to use the various software and testing/ familiarising with the software.
(S1 Week 10) Literature review due: (24/11/2013)	See the lab in action and how the data is taken (may be a different time) Model the surfaces in Vesta. Start analysis of LEED. Hand in literature review.

(S1 Week 1-2)	Finish analysis of LEED and start analysis of XPS. Start preparation for presentation
(S2 Week 3) Presentation: (date TBC)	
(S2 Week 4)	Finish analysis of XPS and start analysis of STM.
(S2 Week 6)	Finish all analysis going over all work done and starting report)
(S2 Week 10): Report due: (26/04/2023)	Hand in report

6.5.3 Risk assessment



RISK ASSESSMENT FORM

School/Department: Physical Sciences	Building: Surface Sciences Lab/Home
Task: Bsc Project: Surface Atomic Structure of Ga3Ni2 and In3Ni2 Intermetallic Catalysts	
Persons who can be adversely affected by the activity: Alfredo Tarttelin	

Section 1: Is there potential for one or more of the issues below to lead to injury/ill health (tick relevant boxes)

People and animals/Behaviour hazards

Allergies	Too few people	Horseplay	Repetitive action	Farm animals
Disabilities	Too many people	Violence/aggression	Standing for long periods	Small animals
Poor training	Non-employees	Stress	Fatigue	Physical size, strength, shape
Poor supervision	Illness/disease	Pregnancy/expectant mothers	Awkward body postures	Potential for human error
Lack of experience	X Lack of insurance	Static body postures	X Lack of or poor communication	Taking short cuts
Children	Rushing	Lack of mental ability	Language difficulties	Vulnerable adult group

What controls measures are in place or need to be introduced to address the issues identified?

Identified hazards	What controls are currently planned or in place to ensure that the hazard identified does not lead to injury or ill-health?	RISK SCORE			Is there anything more that you can do to reduce the risk score in addition to what is already planned or in place?	RESIDUAL RISK SCORE		
		L	C	R		L	C	R
Static body postures	The student may get back pain as most of the project is sat down at a desk, regular breaks are advised.	3	1	3	The student could try to find a standing desk possibly in the library. Stretch regularly and research a better sitting position	2	1	2
Repetitive action	The student will be using a computer for long periods this may lead to hand and finger strain regular breaks are advised.	2	1	2	A hand rest and/or wrist cushion could be used to keep the hands in a more comfortable position.	1	1	1
Lack of experience	The student is inexperienced with the equipment being used and as such will observe a Phd student taking data.	2	1	2	N/A			

L = likelihood; C = consequence; R = overall risk rating

Section 2: Common Workplace hazards. Is there potential for one or more of the issues below to lead to injury/ill health (tick relevant boxes)

Fall from height	Poor lighting	Portable tools	Fire hazards	Chemicals	Asbestos
Falling objects	Poor heating or ventilation	Powered/moving machinery	Vehicles	Biological agents	Explosives
Slips, trips, falls	Poor space design	Lifting equipment	Radiation sources	Waste materials	Genetic modification work
Manual handling	Poor welfare facilities	Pressure vessels	Lasers	Nanotechnology	Magnetic devices
Display screen equipment	Electrical equipment	Noise or vibration	Confined spaces	Gases	Extraction systems
Temperature extremes	Sharps	Drones	Cryogenics	Legionella	Robotics
Home working	Poor signage	Overseas work	Overnight experiments	Unusual events	Community visits
Late/long working	Lack of/poor selection of PPE	Night work	Long hours	Weather extremes	Diving

What controls measures are in place or need to be introduced to address the issues identified?

Identified hazards	What controls are currently planned or in place to ensure that the hazard identified does not lead to injury or ill-health?	RISK SCORE			Is there anything more that you can do to reduce the risk score in addition to what is already planned or in place?	RESIDUAL RISK SCORE		
		L	C	R		L	C	R
Home working	The student may spend most of the time on this project at home. This can lead to limited communication, low motivation and therefore stress. It is advised the student to keep regular contact and try to meet with advisors. The student will be using a computer which can lead to eye strain and headaches. Regular breaks are advised.	3	1	3	The student should try to have regular meeting with the advisors and Phd students, should any issues arise they should try to promptly get support.	2	1	2
Display screen equipment		2	1	2	The student should wherever possible do non-screen work to help the eyes. They should also drink plenty and get fresh air to alleviate headaches.	2	1	2
Long hours	Long hours are very likely for this project as lots of data analysis will need to be done. This can lead to burn out or mental strain. It is advised the student break-up tasks as not to spend too long a period working	4	2	8	The student should set a timer for breaks and speak with the advisor to make a reasonable timeline and how to break-up tasks. The student should also make themselves and other aware of their own limits and stick to these.	2	2	4

Handling of chemicals	The student may encounter handling of chemicals in the lab they should wear all appropriate personal protective equipment where necessary.	2	3	6	N/A		
Handling of Cryogenics	Liquid nitrogen is used in the lab and with the equipment the student should always wear all appropriate personal protective equipment when handling cryogenics.	2	3	6	The student should pour slowly using the correct 'cold traps' and avoid splashing.	1	3
Electrical equipment	There is a risk to electric shock as there are some exposed wires and high voltage supplies to the ultra-high vacuum. The student should assess any risks and not touch anything if they are unsure.	1	4	4	The student should ask about any exposed wires and communicate about equipment in use and where is appropriate to touch and where to avoid when near the equipment.	1	4
Temperature extremes	There is a risk of burns from ovens used in bakeout and from pumps in the lab. The student should not touch any surface they are unsure about, should not touch an oven during bakeout and should wait for the equipment to fully cool down before removing samples from an oven.	2	2	4	N/A		

L = likelihood; C = consequence; R = overall risk rating

Section 3: Additional hazards: are there further hazards **NOT IDENTIFIED ABOVE** that need to be considered and what controls are in place or needed? (list below)



Identified hazards	What controls are currently planned or in place to ensure that the hazard identified does not lead to injury or ill-health?	RISK SCORE			Is there anything more that you can do to reduce the risk score in addition to what is already planned or in place?	RESIDUAL RISK SCORE		
		L	C	R		L	C	R

--	--	--	--	--	--	--	--	--	--

Section 4: Emergency arrangements (List any additional controls that are required to deal with the potential emergency situation)

Emergency situation	Additional control required

Risk assessor (signature).....
Authorised by (signature).....

Date: 09/11/2023
Date: 09/11/2023

Likelihood	Consequence
1 Very unlikely	1 Insignificant – no injury
2 Unlikely	2 Minor – minor injuries needing first aid
3 Fairly likely	3 Moderate – up to seven days absence
4 Likely	4 Major – more than seven days absence; major injury
5 Very likely	5 Catastrophic – death; multiple serious injury

5	5	10	15	20	25
4	4	8	12	16	20
3	3	6	9	12	15
2	2	4	6	8	10
1	1	2	3	4	5
Likelihood					
1	2	3	4	5	

ACTION TO BE TAKEN	
1-4 Acceptable	No further action but ensure controls are maintained
5-9 Adequate	Look to improve at next review.
10-16 Tolerable	Look to improve within specified timescale
17-25 Unacceptable	Stop activity and make immediate improvements

6.6 Presentation questions

Q1. How is the surface annealed? What does the STM image show?

The surface is annealed by ohmic heating where the sample is placed on a sample holder with a heater underneath. Heat is then radiated into the sample holder and brought to a temperature close to the bulk melting point. The surface is not atomically smooth and terminates at planes, the STM images show the surfaces and the layering or 'steps' of these planes.

Q2. Why is the hydrogenation of CO_2 important/interesting?

It is important and interesting as the hydrogenation of CO_2 to ethanol could be a potentially carbon free fuel source and be used in green fuel cells[5]. This is important due to the effects of climate change which are mainly caused by the emission of CO_2 so to create a process by where this could be converted into a fuel source and burned whilst keeping the overall level of CO_2 in the atmosphere the same would be revolutionary. The process does have its hiccups such as it requires hydrogen which can only at the moment be synthesised by processes which are very energy intensive. With majority of energy still being produced by the burning of fossil fuels this poses issues.